MODEL UPDATING OF A MULTI-SPAN HIGHWAY VIADUCT WITH DATA FROM BRIDGE WEIGH-IN-MOTION SENSORS

D. HEKIČ
University of Ljubljana, Faculty of Civil and Geodetic Engineering, Ljubljana, Slovenia
ZAG Ljubljana, Slovenia
Obtained his M.Sc. Eng. at University of Ljubljana, Faculty of Civil and Geodetic Engineering

A. ANŽLIN
ZAG Ljubljana, Slovenia
Obtained his Ph.D. Eng. at University of Ljubljana, Faculty of Civil and Geodetic Engineering

A. ŽNIDARIČ
ZAG Ljubljana, Slovenia
Obtained his Ph.D. at University of Ljubljana, Faculty of Civil and Geodetic Engineering

J. KALIN
ZAG Ljubljana, Slovenia.
Obtained his B.Sc. from University of Ljubljana, Faculty of Mathematics and Physics

P. ČEŠAREK
University of Ljubljana, Faculty of Civil and Geodetic Engineering, Ljubljana, Slovenia
Obtained his Ph.D. at University of Ljubljana, Faculty of Civil and Geodetic Engineering

Abstract

Traditionally, finite element model updating (FEMU) of bridges is based on measured modal parameters and occasionally on measured structural response under known loads. Until recently, strain measurements from sensors installed for weighing vehicles with bridge weigh-in-motion (B-WIM) systems haven't been used for the FEMU. A multi-span concrete highway viaduct renovated between 2017 and 2019 and equipped with over 200 sensors and a B-WIM system showed the potential to develop the FEMU concept using B-WIM data. This study compares the maximum longitudinal strains in the most heavily instrumented span, induced by full-speed calibration vehicle passages, with modelled strains. Three variables were updated based on the sensitivity study results: Young's modulus adjustment factor of all structural elements and two anchorage reduction factors that considered the interaction between the superstructure and non-structural elements. The analysis highlighted the importance of initial manual FEMU to reflect non-structural elements during automatic non-linear optimisation accurately and demonstrated a successful use of pseudo-static B-WIM loading data in the FEMU process. The study also suggested extending this approach to using random B-WIM-weighed vehicles for long-term monitoring of load-dependent phenomena and long-term monitoring of structural parameters.

Keywords: Bridge weigh-in-motion (B-WIM), Monitoring, Bridge, Structural health monitoring (SHM), Finite element model updating (FEMU)

1. Introduction

Maintaining bridge performance at desired levels is becoming challenging because traffic infrastructure is ageing (ASCE, 2021) and increasingly important because passenger and freight traffic is expected to increase by more than 230 % between 2015 and 2050 (Forum, 2021). Therefore, new innovative methods and technologies are developed and implemented to enable infrastructure managers to monitor their assets. One such method is the bridge weigh-in-motion (B-WIM) system used beyond its primary weighing function to update the finite element (FE) model. By enhancing B-WIM to monitor the state of structures, this technology is making progress towards digital twin capabilities, allowing for continuous observation of instrumented structures over their lifetime. Furthermore, such technology would also allow using structural health monitoring (SHM) not only for large but also for short and medium-span bridges.

Implementing a damage detection strategy, commonly known as SHM (Farrar and Worden, 2012), became prevalent following the widespread availability of computers that enabled the large-scale collection of measured data. One of the first SHM studies on bridges was conducted by Cantieni (1984), while Rytter (1993) laid the foundation for the assessment of damage to engineering structures based on vibration measurements, followed by a steep rise in SHM development. At the turn of the millennium, Ko and co-authors (1999) presented the most comprehensive SHM on bridges in the world at that time. In the last 20 years, the SHM field has grown considerably, reflected in an increasing number of papers, manuscripts, results of multi-year measurements and developed methods for damage detection, with the most recent high-profile studies focusing on machine learning techniques.

Since its early beginnings (Moses, 1979), the accuracy of the B-WIM field has significantly improved. The replacement of the analytical by the measured influence line (Žnidarič, Lavrič and Kalin, 2002; OBrien, Quilligan and Karoumi, 2005) made a significant contribution. As the influence line is a structural parameter, it can be monitored in the time domain, as conceptually presented by Cantero and González (2015) and more recently by Heitner et al. (2020). Žnidarič and Kalin (2020) introduced the parameterised influence line, where influence lines are calculated from random vehicles rather than vehicles of known characteristics only. Overall three so-called performance indicators (PI), which relate to the response of the structure under traffic load, can be extracted from the B-WIM measurements: influence line, dynamic amplification factor (DAF) and lane or girder distribution factor (GDF). These parameters help bridge engineers to analyse the reliability of bridges by using realistic traffic loads and structural responses rather than assumed ones.

FEMU involves the use of SHM measurements. Therefore, these two areas have developed in parallel. Most bridge FEMU studies are based on measured modal parameters (dynamic SHM) and less frequently on measured structural response under known load (static or quasi-static SHM), the latter being more expensive and time-consuming. No studies were found in which data from strain sensors installed primarily for B-WIM measurements are used to update the FE model of a viaduct.

This paper describes a viaduct installed with permanent monitoring and B-WIM systems. The longitudinal strains caused by calibration vehicles, measured in the most heavily instrumented span, were statistically processed and used in a FEMU study. After sensitivity study and manual FEMU, three parameters were updated: Young's modulus adjustment factor of all structural elements and two anchorage reduction factors that considered the interaction between the superstructure and non-structural elements. Automatic FEMU was performed finally, utilising a non-linear optimisation algorithm, which revealed the increase of the design value of Young's modulus and non-negligible contribution of safety barriers.

2. Case study viaduct

The case study viaduct consists of two parallel structures with an overall length of 588 m and 544 m. The right structure in Figure 1 (a) has 17 spans and carries the traffic in the southwest direction. The most heavily instrumented span (14^{th} in line, in the traffic direction) is the subject of this paper. The left structure has 15 spans and carries the traffic in the opposite direction. Figure 1 (b) shows the view of the support structure.

(a) **(b)**

Figure 1 – Case study viaduct: (a) View from above; (b) View from below

The viaduct is strategically located on the heavily trafficked 5^{th} Trans-European corridor from Venice in Italy to Lviv in Ukraine. It crosses twice a double-track railway line and twice a state road. Overall nearly 49.000 vehicles over 3.5 tonnes and, among those, nearly 36.000 vehicles over 7.5 tonnes were weighed on the right structure in November 2018. Figure 2 shows a histogram of gross vehicle weight (GVW) for vehicles over 7.5 tonnes weighed in this period.

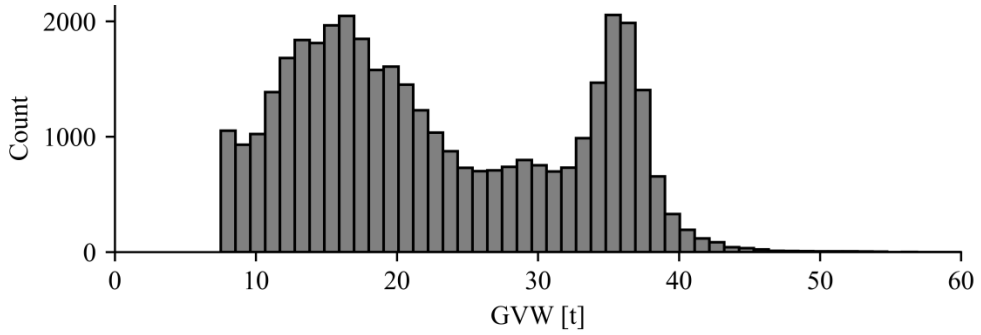

Figure 2 – Gross vehicle weight (GVW) histogram for vehicles over7.5 t in the driving lane for November 2018

The viaduct underwent four renovations after its completion in 1972. During the most recent reconstruction period from 2017 to 2019, the viaduct owner decided to permanently monitor certain critical performance parameters. More than 200 sensors were installed to measure the strains on the main girders and the carbon rods used for the bridge deck extensions, pier caps, vibrations of the external tendons and temperature. A part of the installation was a B-WIM system, which uses the data from longitudinal strain measurements on the main girders in the most heavily instrumented span.

3. Processing of the measurements

In November 2018, the B-WIM system was calibrated with three calibration vehicles: V1 (24.1 t, axle disposition 12), V2 (39.0 t, axle disposition 113) and V3 (39.6 t, axle disposition 122). Each passed the considered span 20 times in the driving lane and 20 times in the overtaking lane. Calibration was performed during free traffic flow, with a mean speed of 77 km/h. There was only one calibration vehicle on the measured bridge span. A car was driving behind the last calibration vehicle to prevent others from following too closely or even overtaking them.

Among those passages, the ones with excessive deviation in the transverse position or simultaneous presence of another vehicle were not considered. Finally, time domain signals of 16, 17 and 18 calibration vehicles V1, V2 and V3 passages, respectively, were selected for the FEMU. Only passages on the driving lane were considered in this study. Figure 3 (a) shows GVWs for vehicles between 3.5 t and 80 t in November 2018. It can be seen that the traffic structure is comparable across all weeks, with white spots indicating Sundays when the ban on heavy vehicles in Slovenia applies. In the detailed view in Figure 3 (b), the red dots indicate the calibration vehicles V1, V2 and V3.

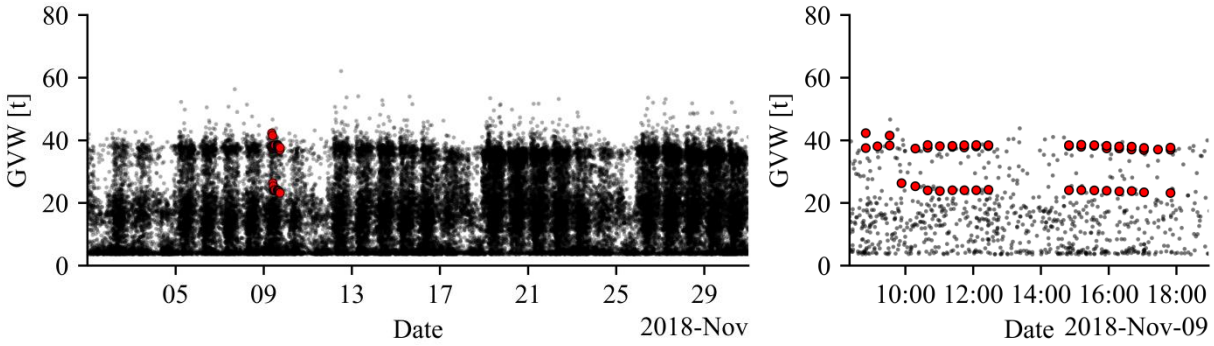

Figure 3 – GVWs for vehicles over 3.5 t in the driving lane in November 2018 (a) and 9th November 2018 (b), with calibration vehicle runs (red colour dots)

After time-domain signals were selected, post-processing followed. Each time-domain signal was filtered with a 2 Hz low-pass filter to eliminate the dynamic component (Kalin *et al.*, 2021), approximating the response under pseudo-static load. The maximum values of the pseudo-static responses were then identified for all signals. The considered span (and all other spans of the viaduct) has 4 longitudinal girders (marked as MG1, MG2, MG3 and MG4 in the legend in Figure 4 (b)). B-WIM system uses data from strain-gauge sensors mounted at the mid-span of those girders. Several strain gauges were installed close to each other to ensure robust measurements, three at the MG2, MG3 and MG4, and two at the MG1 location. The sensors in Figure 4(b) are labelled as "SG_0g-n", where g denotes the girder index and n denotes the index of the strain gauge sensor on that particular girder.

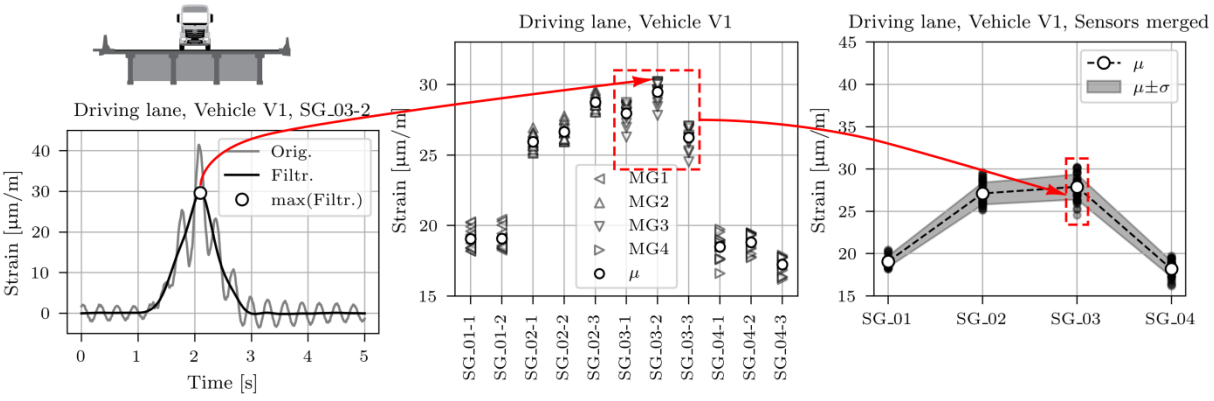

Figure 4 – Process of determining the mean (μ) and standard deviation (σ) strain for the passage of vehicle V1: (a) Time domain signal of SG-03-02; (b) Maximum values for all passages and individual sensors; (c) Maximum values for all passages and sensors grouped according to considered girders

After maximum values were identified for all sensors and for all passages, the values corresponding to the sensor on the same girder were combined, and their mean value and

standard deviation were calculated. Finally, four mean and four standard deviation values were calculated for each calibration vehicle and were used in the following for the FEMU. Figure 4 shows the workflow for measurement processing for vehicle V1. The same approach was used for vehicles V2 and V3.

4. Finite element model updating (FEMU)

Abaqus CAE 2016 ('DS SIMULIA, 2016) FE analysis software in conjunction with Python 3 (Python Software Foundation, 2023) and *scipy* library (Virtanen *et al.*, 2020) was employed to update the FE model of the analysed span. Detailed model description, sensitivity analysis and the entire update process are beyond the scope of this paper. The interested reader is referred to the article (Hekič *et al.*, 2023).

Figure 5 (a) presents the FE model, which consists of roughly 20.000 C3D20R-type finite elements with an approximate global size of 0.5 m.

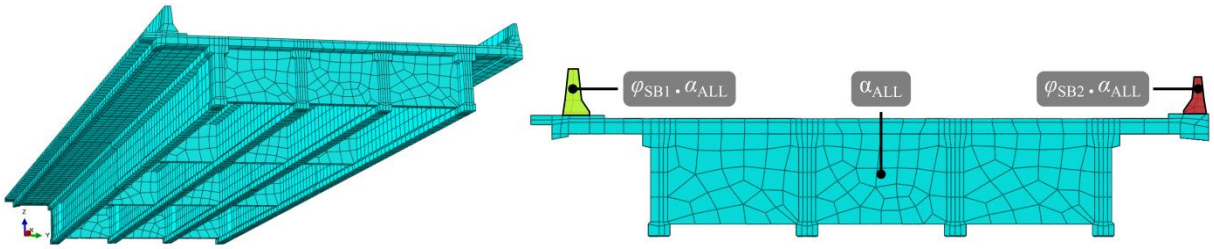

(a) **(b)**

Figure 5 – 3D view of the FE model (a) and section cut view (b) of the FE model with notations of the elements to which variables α_{ALL}, φ_{SB1}, φ_{SB2} are updated

The global size of the finite elements was determined based on the convergence study (Figure 6), where average strains SG_01, SG_02, SG_03 and SG_04 were calculated for different sizes of the finite elements under point load of 10 kN at the mid-span.

The FE model consists of eight different structural elements/groups of structural elements: Slab, external main girders, internal main girders, cross girders, safety barrier 1, safety barrier 2, edge beams and asphalt. Each of those elements has defined unique material properties, i.e. different Young's modulus and Poisson ratio, according to the design documentation (Cestni sklad (1972), DARS (2019)). Elastomeric bearings were modelled as springs, with the vertical, translational, and rotational stiffness assumed from the design documentation data. The influence of neighbouring spans was accounted for with boundary conditions set on the surface, which cut the considered span from the entire structure.

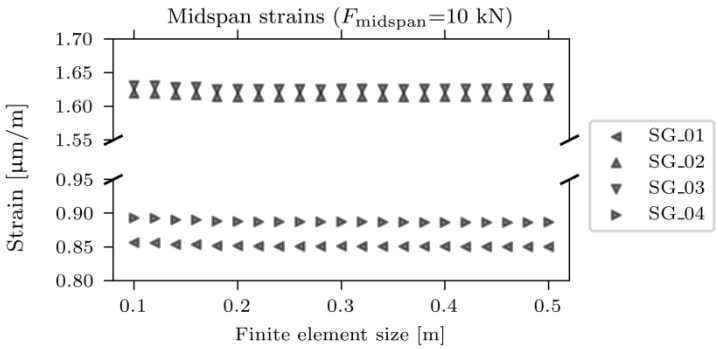

Figure 6 – Results of the FE convergence study

Usually, when performing load tests for the FEMU (Schlune, Plos and Gylltoft, 2009), the type and disposition of the sensors are tailored such that the updated material property or boundary condition (variables) are sensitive to the measured response. On the contrary, this study aimed to investigate to what extent the strain-gauge sensors, primarily installed for B-WIM purposes, can be used for FEMU. It was, therefore, crucial to perform extensive sensitivity analysis, which ranked the structural elements by the sensitivity of the mid-span strains under calibration vehicles to their Young's modulus. For the bridge bearing stiffness, it was found to be insensitive, while for structural elements, it was decided to update three variables: α_{ALL}, φ_{SB1} and φ_{SB2}. α_{ALL} is Young's modulus adjustment factor of all structural elements, and could be interpreted as a global stiffness increase factor. φ_{SB1} and φ_{SB2} are anchorage reduction factors, which consider the reduced contribution of safety barriers 1 and 2 to the superstructure stiffness. They are attached to the deck through the anchoring plate (safety barrier 1) and directly through the anchors (safety barrier 2). Within the FEMU, as seen in Figure 5 (b), all structural elements had Young's modulus varied by the same adjustment factor, and Young's modulus of both safety barriers was additionally multiplied by the anchorage reduction factors.

Within the FEMU, modelled strains were compared with the maximum measured (pseudo-static) longitudinal mid-span strains under calibration vehicles and their difference was minimised. The process of determining the maximum measured strains is described in Section 3. An additional procedure was performed to get the maximum modelled strains, where the position of each calibration vehicle, approximated as a series of point loads, was varied along the considered span to get the maximum strains. Once a position for all three calibration vehicles resulting in the greatest strains at sensor locations was determined, this position was used for all further FEMU studies. Mid-span strains proved to be very sensitive to the vehicle position. Therefore, care should be taken to estimate the position correctly.

The job of the objective function is to combine measured and modelled responses. This study used the sum of squared relative differences with standard deviation as a normalisation term (Schlune, Plos and Gylltoft, 2009). The objective function used in this study (1) was slightly modified to consider average values.

$$\mathrm{J} = \sum_{v=1}^{n_v} \sum_{g=1}^{n_g} \frac{\left(\mathrm{z}_{\mathrm{num},v,g} - \mathrm{z}_{\mathrm{exp},v,g}\right)^2}{{\sigma_{\mathrm{exp},v,g}}^2} \tag{1}$$

where $z_{num,v,g}$ and $z_{exp,v,g}$ were calculated as:

$$z_{num,v,g} = \frac{1}{n_{g,s}} \sum_{s=1}^{n_{g,s}} \varepsilon_{num,v,g,s}\,(\alpha_{ALL}, \varphi_{SB1}, \varphi_{SB2}) \text{ and} \quad (2)$$

$$z_{exp,v,g} = \frac{1}{n_{g,s}} \sum_{s=1}^{n_{g,s}} \left(\frac{1}{n_{v,p}} \sum_{p=1}^{n_{v,p}} \varepsilon_{exp,v,g,s,p} \right). \quad (3)$$

- v denotes the calibration vehicle index;
- n_v denotes the number of calibration vehicles considered (3 in this study);
- g denotes the main girder index;
- n_g denotes the number of main girders considered (4 in this study);
- $\sigma_{exp,v,g}$ denotes the standard deviation of measured strains for main girder g and vehicle v;
- s denotes the strain gauge sensor index on the selected main girder;
- $n_{g,s}$ denotes the number of strain gauges considered in a given girder g (2 or 3 in this study);
- p denotes the passage index of the selected calibration vehicle;
- $n_{v,p}$ denotes the number of vehicle v passages;
- $\varepsilon_{num,v,g,s}$ denotes the FE model longitudinal strain, oriented parallel to the longitudinal direction of the viaduct, in the selected node that corresponds to the s-th strain gauge sensor on the g-th main girder, caused by the v-th calibration vehicle positioned on the location that results in the maximum strain at sensors SG_0g ;
- $\varepsilon_{exp,v,g,s,p}$ denotes the maximum measured longitudinal strain in the s-th strain gauge sensor on the g-th main girder caused by the v-th calibration vehicle during p-th passage.

Non-linear optimisation utilised sequential least squares programming (SLSQP) algorithm (Kraft, 1988) from *scipy* (Virtanen *et al.*, 2020) library, which found the optimum solution in 61 steps. Table 1 presents the optimisation results. The algorithm found the optimum values of the α_{ALL} to be 1.25, safety barrier 1 to have a negligible contribution (φ_{SB1} = 0) and safety barrier 2 to have a non-negligible contribution (φ_{SB1} = 0.56) to the stiffness of the superstructure.

Table 1 – Results of the non-linear optimisation for three variables: α_{ALL}, φ_{SB1}, φ_{SB2}

Value of the objective function	10.23
α_{ALL} (Young's modulus adjustment factor of all elements)	1.25
φ_{SB1} (SB1 anchorage reduction factor)	0.00
φ_{SB2} (SB2 anchorage reduction factor)	0.56
$\alpha_{ALL} \cdot \varphi_{SB1}$	0.00
$\alpha_{ALL} \cdot \varphi_{SB2}$	0.70

Figure 7 compares the measured and modelled maximum strains before and after FEMU. Strains of the initial FE model, which strictly follows the material characteristic from the design documentation and ignores the safety barriers, are shown in blue. The red line corresponds to the FE model after FEMU. From the figure, the initial FE model strain values are clearly overestimated.

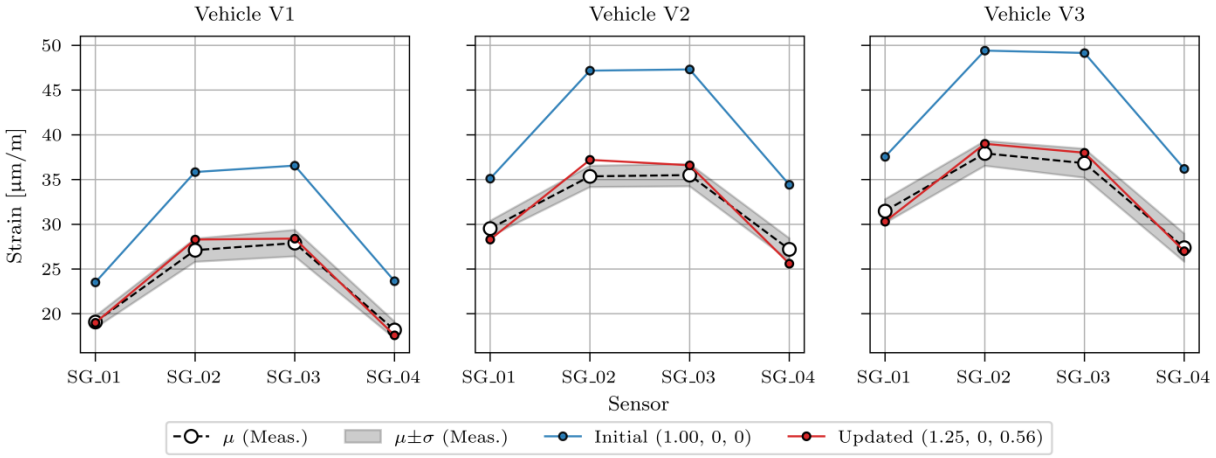

Figure 7 – Comparison of the maximum measured and modelled strains before and after FEMU (values in bracket indicating α_{ALL}, φ_{SB1} and φ_{SB2})

It should be noted that converged values for the anchorage reduction factors φ_{SB1} and φ_{SB2} should not be treated as final structural properties. Safety barriers are mounted to the superstructure at discrete locations, whereas the interaction (friction) of the remaining part of the contact surface depends on the deformation of the deck, i.e. the contribution of the safety barriers to the bending stiffness of the superstructure is load dependant. This realisation is important when viaduct is considered in the limit states where the influence of the safety barriers is expected to be negligible.

The primary advantage of combining B-WIM and FEMU lies in the multiple uses of sensors: to monitor the traffic load and the response of the bridge to external actions (traffic, temperature and other loads). This enables to monitor the structural behaviour of considered elements of the bridge. Nonetheless, there are limitations in the number, arrangement, and type of sensors that may not always be optimal for both B-WIM and SHM applications.

5. Conclusions

This paper presents the concept of using data from B-WIM sensors for FEMU. Utilising sensitivity study, manual and automatic non-linear FEMU, it was possible to update the FE model with 3 variables: Young's modulus adjustment factor of all structural elements and anchorage reduction factors of both safety barriers.

The updated FE model reduced the bending strains under calibration vehicles by about 25%. In addition, the results confirmed that the safety barriers non-negligibly contributed to the global stiffness of the superstructure. However, the latter is only true for the considered load levels, and contribution of the safety barriers to the bending stiffness of the span may become insignificant at higher load levels.

This study was based on B-WIM data for calibration vehicles. In future, the FE model updating will be extended with B-WIM data for random vehicles and higher load levels.

6. Acknowledgement

The authors would like to express their gratitude to the Motorway Company of the Republic of Slovenia (DARS d.d.), for providing the results from the long-term monitoring of the Ravbarkomanda viaduct. The authors would also like to acknowledge company CESTEL d.o.o. for their B-WIM-related support.

The authors acknowledge the financial support from the Slovenian Research Agency (Young Researcher funding program (ARRS No. 53694), research core funding No. P2-0260 and P2-0273 and infrastructure program No. I0-0032).

7. References

- ASCE (2021) "Structurally Deficient Bridges | Bridge Infrastructure | ASCE's 2021 Infrastructure Report Card", pp. 18–25. Available at: https://infrastructurereportcard.org/cat-item/bridges/.
- Cantero, D. and González, A. (2015), "Bridge Damage Detection Using Weigh-in-Motion Technology", Journal of Bridge Engineering, 20(5), p. 04014078. Available at: https://doi.org/10.1061/(asce)be.1943-5592.0000674.
- Cantieni, R. (1984), "Dynamic load tests on highway bridges in Switzerland – 60 Years experience of EMPA". Dübendorf, Switzerland: Swiss Federal Laboratories for Materials Testing and Research.
- Cestni sklad SRS (1970), "Technical report about the general project of the Ravbarkomanda viaduct" (in Slovene).
- DARS (2019), "VA0174 Ravbarkomanda viaduct rehabilitation plan: Notebook 3/1.1-General part, technical part" (in Slovene).
- DS SIMULIA Abaqus 2016, "Documentation". Available at: http://130.149.89.49:2080/v2016/index.html.
- Farrar, C.R. and Worden, K. (2012), "Structural Health Monitoring: A Machine Learning Perspective, Structural Health Monitoring: A Machine Learning Perspective". Available at: https://doi.org/10.1002/9781118443118.
- Forum, IT (2021), "ITF Transport Outlook 2021". Available at: https://doi.org/https://doi.org/https://doi.org/10.1787/16826a30-en.
- Heitner, B., Schoefs, F., OBrien, E.J., Žnidarič, A. and Yalamas, T. (2020), "Using the unit influence line of a bridge to track changes in its condition", Journal of Civil Structural Health Monitoring, 10(4), pp. 667–678. Available at: https://doi.org/10.1007/s13349-020-00410-7.
- Hekič, D., Anžlin, A., Kreslin, M., Žnidarič, A. and Češarek, P. (2023), "Model Updating Concept Using Bridge Weigh-in-Motion Data", Sensors. Available at: https://doi.org/10.3390/s23042067.
- Kalin, J., Žnidarič, A., Anžlin, A. and Kreslin, M. (2021), "Measurements of bridge dynamic amplification factor using bridge weigh-in-motion data", Structure and Infrastructure Engineering, 0(0), pp. 1–13. Available at: https://doi.org/10.1080/15732479.2021.1887291.

- Ko, JM, Ni, YQ and Chan, T.H.T. (1999), "Dynamic monitoring of structural health in cable-supported bridges", in Proceedings of SPIE - The International Society for Optical Engineering, pp. 161 – 172. Available at: https://www.scopus.com/inward/record.uri?eid=2-s2.0-0032674617&partnerID=40&md5=f4af54f0d564da0fce16f13c906a986f.
- Kraft, D. (1988), "A Software Package for Sequential Quadratic Programming". Weissling.
- Moses, F. (1979), "Weigh-in-motion system using instrumented bridges", Journal of Transportation Engineering, 105(3).
- OBrien, E., Quilligan, M.J. and Karoumi, R. (2005), "Calculating an Influence Line from direct measuremetns", Proceedings of the Institution of Civil Engineers, Bridge Engineering 159(1), pp. 31–34.
- Python Software Foundation (2023), "Python 3.7.16 Documentation, The Python Language Reference". Available at: https://docs.python.org/3.7/reference/ (Accessed: 31st March 2023).
- Rytter, A. (1993), "Vibrational Based Inspection of Civil Engineering Structures". Dept. of Building Technology and Structural Engineering, Aalborg University.
- Schlune, H., Plos, M. and Gylltoft, K. (2009), "Improved bridge evaluation through finite element model updating using static and dynamic measurements", Engineering Structures, 31(7), pp. 1477–1485. Available at: https://doi.org/https://doi.org/10.1016/j.engstruct.2009.02.011.
- Virtanen, P., Gommers, R., Oliphant, T.E., Haberland, M., Reddy, T., Cournapeau, D., Burovski, E., Peterson, P., Weckesser, W., Bright, J., van der Walt, S.J., Brett, M., Wilson, J., Millman, K.J., Mayorov, N., Nelson, A.R.J., Jones, E., Kern, R., Larson, E., Carey, C.J., Polat, \.Ilhan, Feng, Y., Moore, E.W., VanderPlas, J., Laxalde, D., Perktold, J., Cimrman, R., Henriksen, I., Quintero, E.A., Harris, C.R., Archibald, A.M., Ribeiro, A.H., Pedregosa, F., van Mulbregt, P. and SciPy 1.0 Contributors (2020), "{SciPy} 1.0: Fundamental Algorithms for Scientific Computing in Python", Nature Methods, 17, pp. 261–272. Available at: https://doi.org/10.1038/s41592-019-0686-2.
- Žnidarič, A. and Kalin, J. (2020), "Using bridge weigh-in-motion systems to monitor single-span bridge influence lines", Journal of Civil Structural Health Monitoring, 10(5), pp. 743–756. Available at: https://doi.org/10.1007/s13349-020-00407-2.
- Žnidarič, A., Lavrič, I. and Kalin, J. (2002), "The Next Generation of Bridge Weigh-in-Motion Systems", in 3rd International Conference on Weigh-in-Motion (ICWIM3). 3rd International Weigh-in-motion conference.